https://doi.org/10.5194/egusphere-2025-156
Preprint. Discussion started: 7 March 2025

Title: Extreme carbon fluxes may result from autochthonous particulate organic carbon regulated by the interactions between picophytoplankton and heterotrophic bacteria in river-reservoir systems

Authors: Fang Luo [1,2,3], Zhe Li [2,3], Qiong Tang [1,2,3], Yan Xiao [2,3], Lunhui Lu [2,3], Dianchang Wang [4], Chong Li [4], and Xinghua Wu [4]

Affiliations:

[1] Key Laboratory of Hydraulic and Waterway Engineering of the Ministry of Education, Chongqing Jiaotong University, Chongqing, 400074, China

[2] CAS Key Lab of Reservoir Environment, Chongqing Institute of Green and Intelligent Technology, Chinese Academy of Sciences, Chongqing, 400714, China

[3] College of Resources and Environment, Chongqing School, University of Chinese Academy of Sciences, Chongqing, 400714, China

[4] China Three Gorges Corporation, Wuhan, 430010, China

Correspondence: Zhe Li (lizhe@cigit.ac.cn)

https://doi.org/10.5194/egusphere-2025-156
Preprint. Discussion started: 7 March 2025

Abstract

Freshwater is a significant natural source of atmospheric methane (CH_4) and carbon dioxide (CO_2) while also receiving significant amounts of particulate organic carbon (POC) from various origins. The variation in carbon (CH_4 and CO_2) fluxes in freshwater systems is heavily influenced by the sources of POC. The trophic interaction between picophytoplankton (PP) and heterotrophic bacteria (HB) plays a vital role in the carbon cycle within the aquatic system. However, the contributions of different sources of POC to the concentrations and fluxes of CH_4 and CO_2 are still unclear. Here, we explored the contribution of POC from different sources to extreme carbon emission and the interaction between PP and HB. The evidence from isotope analysis further proved that the extreme carbon fluxes were strongly influenced by autochthonous POC rather than allochthonous POC. Network analysis showed that the positive interaction strength between phytoplankton and bacterioplankton in extreme carbon groups was higher than in normal carbon groups. The results of the structure equation modeling analysis also highlighted that the PP-HB interaction strongly drove the extreme carbon values. This study first introduced the probability statistics method to identify and classify high or low extreme carbon values. These findings also highlight the importance of PP and HB in carbon extreme emissions, and we hope our study can provide an important implication for integrating PP-HB interaction into predicting extreme carbon emissions in the river-reservoir ecosystem.

Keywords: Organic carbon; Autochthonous; Allochthonous; Picophytoplankton; Methane emissions

https://doi.org/10.5194/egusphere-2025-156
Preprint. Discussion started: 7 March 2025

1. Introduction

Freshwaters are considered important sources of greenhouse gases (GHGs) to the atmosphere (Bauduin et al., 2024). According to estimates in the Sixth Assessment Report by the Intergovernmental Panel on Climate Change (IPCC), annual global CH_4 and CO_2 emissions from freshwaters are estimated to be approximately 1.5 Pg CO_2 and 159 Tg CH_4 (IPCC, 2021), offsetting approximately 25% of the terrestrial carbon sink (Emilson et al., 2018). However, these estimates have a high degree of uncertainty, mainly due to the apparent spatiotemporal heterogeneity and variability of CH_4 and CO_2 fluxes across the air-water interface. Thus, it is crucial to reduce these uncertainties in emission estimation from a local to a global scale by improving the understanding of fluctuations in CH_4 and CO_2 concentrations and air-water fluxes.

There have been extensive studies on the cause of significant fluctuations in freshwater CH_4 and CO_2 fluxes. The hydrological and hydrodynamic conditions, such as river flow, drought, or floods, are significant factors that regulate this variability. Additionally, meteorological factors like short-term heavy precipitation and winds are non-negligible and significant physical factors causing the large variability of freshwater CH_4 and CO_2 fluxes (Wang et al., 2008). The physical disturbances not only affect the intensity of turbulence mixing at the air-water interface, which changes the rate of air-mass transfer, but also trigger significant input of terrigenous organic carbon (OC) and essential nutrients into freshwater, leading to increased CH_4 and CO_2 emissions (Liikanen et al., 2002). For example, the decomposition of a significant input of terrigenous OC in the littoral area of freshwater might lead to the ebullition

https://doi.org/10.5194/egusphere-2025-156
Preprint. Discussion started: 7 March 2025

emission of CH_4 in the summer. On the other hand, ecosystem-level events significantly result in extreme values of CH_4 and CO_2 fluxes as well. The air-water CH_4 flux was expected to exhibit extremely high values during algal blooms, concurrently with low levels of surface water CO_2 concentrations, leading to an apparent CO_2 sink during the blooming period (Sun et al., 2021). It appeared plausible that several ecological factors or processes could contribute to the occurrence or outbreaks of these high or low extremes of CH_4 and CO_2 concentrations in surface water and their air-water fluxes. Yet, compared with the physical processes, how ecological factors or processes could trigger extreme C emissions in freshwaters are not frequently addressed. New mechanisms are needed to be elucidated.

The minor component of the planktonic communities (Stockner and Antiam, 1986), the picoplankton (defined by a cell size of 0.2-2 μm) (Sieburth et al., 1978), mainly includes autotrophic picophytoplankton and heterotrophic bacteria (Stockner, 1988). Picophytoplankton are active and critical primary producers in aquatic ecosystems due to their wide distribution, rapid growth rates, and metabolic capabilities (Stockner, 1988). In the ocean, picophytoplankton can contribute 50-90% of primary productivity (Poulton et al., 2006), significantly providing autochthonous organic carbon to the aquatic ecosystem. Especially during an algal bloom, small-sized phytoplankton, such as picophytoplankton, can fix more CO_2 through photosynthesis. This is because picophytoplankton have higher growth rates and are more effective in nutrient and light acquisition than larger phytoplankton (Irion et al., 2021). Research in the past decade has also shed new light on a large proportion of

https://doi.org/10.5194/egusphere-2025-156
Preprint. Discussion started: 7 March 2025

tiny picophytoplankton to carbon export, especially in oligotrophic oceans (Richardson, 2019). On the other hand, heterotrophic bacteria decompose organic carbon, transferring different sources of OC into CH_4 or CO_2 (Guillemette et al., 2013). It was reported that heterotrophic bacteria can consume 20-60% of the total primary production (Williams, 1981). The effects of heterotrophic bacteria on CH_4 or CO_2 emissions are strongly dependent on the decomposition of organic carbon with different bioavailability (Grasset et al., 2018). Therefore, as an important part of the planktonic communities, picophytoplankton and heterotrophic bacteria undoubtedly are essential components for understanding the carbon cycle in the aquatic ecosystem.

Interactions between picophytoplankton and heterotrophic bacteria are critical for exploring the possible mechanisms that regulate CH_4 and CO_2 dynamics in aquatic ecosystems. Picophytoplankton and heterotrophic bacteria do not exist in isolation (Faust and Raes, 2012), and there are complex ecological interactions between them, which span mutualism, commensalism, parasitism, and competition (Seymour et al., 2017). In brief, the relationship between picophytoplankton and heterotrophic bacteria is based on resource provision and can be either cooperative (exchange of resources) or competitive (competition for resources) (Amin et al., 2012). Mutualism, a win-win relationship, is found to be the primary relationship between these two microorganisms (Zhang et al., 2021). One example for mutualism is cross-feeding, in which two species exchange metabolic products to facilitate the growth of both (Woyke et al., 2006). For instance, heterotrophic bacteria directly obtain a large proportion of picophytoplankton-derived organic carbon to meet their carbon demand

https://doi.org/10.5194/egusphere-2025-156
Preprint. Discussion started: 7 March 2025

(Zhou et al., 2022). Autrophic picophytoplankton can utilize vitamins and micronutrients (that is, iron, copper, etc.) released by heterotrophic bacteria (Zhou et al., 2022; Durham et al., 2015). There are two possible mechanisms by which picophytoplankton-heterotrophic bacteria interactions affect CH_4 and CO_2 flux. First, the cooperative relationship between picophytoplankton and heterotrophic bacteria produces strong coupling and positive feedback between these two organisms, increasing microbial metabolic efficiency and full utilization of OC (Coyte et al., 2015). Second, "physical interactions" between picophytoplankton and heterotrophic bacteria in an extracellular microenvironment (that is, "phycosphere") mediate the level of aggregation of picophytoplankton biomass, which manipulates downward C flux (Seymour et al., 2017). Despite their small size, more than 40% of *Synechococcus* cells were found to be conjoint with heterotrophic bacteria ("physical interaction") in situ observation (Malfatti and Azam, 2009). Such an increase in picophytoplankton and heterotrophic bacteria cell aggregation mediated by interactions between picophytoplankton and heterotrophic bacteria, especially during the algal blooms, would lead to an increase in the carbon flux exported to the bottom water column (Gärdes et al., 2011), thus offering more substrate for CH_4 production. In recent years, the influence of picophytoplankton and heterotrophic bacteria on the biogeochemical cycle of carbon has been widely discussed in marine ecosystems (Zhou et al., 2022). Little is known about the dynamics of CH_4 and CO_2 production and emissions driven by the interaction of these "specific participants" in freshwaters.

https://doi.org/10.5194/egusphere-2025-156
Preprint. Discussion started: 7 March 2025

River damming disrupts the natural connectivity of rivers and causes a shift in the aquatic system from lotic to lentic type along the longitudinal gradients towards the dam site (Baxter, 1977). This change significantly affects the river's flow by reducing speed, prolonging the hydraulic retention time, and interrupting sediment movement (Maavara et al., 2020). Reservoirs receive a higher input of terrigenous organic carbon than natural lakes due to their comparably lower ratio of watershed area to surface area and higher shoreline development (Thornton et al., 1990). Over the past two decades, there has been increasing concern about the excessive carbon emissions from reservoirs. This is significant for global carbon biogeochemical cycles and has implications for the hydropower industry. However, organic carbon sources contributing to carbon emission, especially extremes, have yet to be well explored. This lack of understanding hinders the accurate prediction of reservoir carbon emissions in various scenarios.

Although extremely high or low CH_4 and CO_2 concentrations in surface water or their air-water fluxes were not frequently detected, it was assumed that the extremes or normal status of C fluxes could represent the distinctive ecosystem-level state and the biogeochemical cycling. Thus, processes and mechanisms of carbon cycling in the river-reservoir system could be further explored through the categorization of extreme or normal status of CH_4 and CO_2 concentrations or air-water fluxes. Therefore, we hypothesized that (1) autochthonous organic carbon (OC) in river-reservoir systems greatly contributes to the occurrences of extreme values of CH_4 and CO_2 concentrations; (2) terrigenous OC contributes to the normal values of CH_4 and CO_2

https://doi.org/10.5194/egusphere-2025-156
Preprint. Discussion started: 7 March 2025

concentrations; and (3) The interaction of autotrophic picophytoplankton (PP) and heterotrophic bacteria (HB) could be intensified with an increase in trophic state, thus promoting the production of extreme values of CH_4 and CO_2.

To test the hypothesis, we first identified and classified extremely high or low values of CH_4 and CO_2 concentrations and their air-water fluxes across different types of reservoirs in the upper Yangtze River basin in China. Then, we investigated variations and interactions of picophytoplankton and heterotrophic bacteria, together with environmental parameters and stable isotopic evidence. Building on our sampling campaign (Tang et al., 2023), we restructured the information and conducted new analyses. This study enhances prior research through two key contributions:

1) We categorized the concentrations and fluxes of CH_4 and CO_2 from the previous datasets into two groups: extreme and normal. This classification is based on the probability of occurrence and offers new insights into the mechanisms that regulate these gases.

2) We included new data from pico-phytoplankton and heterotrophic bacteria. This information may provide fresh evidence regarding the interactions between phytoplankton and bacteria that contribute to CH_4 emissions in the extreme group.

Hopefully, our study will determine the role of picophytoplankton and heterotrophic bacteria in extreme carbon emissions, which would yield new insights into extreme carbon emissions with the two tiny planktonic communities in river-reservoir systems.

https://doi.org/10.5194/egusphere-2025-156
Preprint. Discussion started: 7 March 2025

2. Materials and methods

2.1. Study sites and sample collection

Five reservoirs in the upper Yangtze River basin were selected (Fig. 1), including Xiluodu (XLD), Xiangjiaba (XJB), Shizitan Reservoir (SZT), Xiaoba II (XB II) and Three Gorges Reservoir (TGR). Among these five reservoirs, XLD, XJB, and TGR are located on the main stem of the Yangtze River, which are large river-valley dammed cascade reservoirs and mainly serve as hydropower generation and flood control. The SZT (also known as Changshou Lake) is located on the Longxi River, a tributary of the Yangtze River, and functions as tourism now. XB II (with a total capacity of 11300 m^3) is a small reservoir only for drinking water supply located on a tertiary tributary named Ganxi Gulley of the Yangtze River. The geographical and project information of these selected reservoirs is described in Table S1.

Sampling campaigns were conducted in May, July, and November 2019 to obtain a representative dataset containing different seasons. Twenty-six sampling sites were set in the five selected reservoirs, covering the riverine zone, transitional zone, and lacustrine zone of each reservoir (Fig. 1; Table S2). Water samples for cell enumeration of picophytoplankton and heterotrophic bacteria were filtered through a 50-μm nylon sieve. The filtered samples were immediately fixed by glutaraldehyde solution and kept at -80 °C in the laboratory until analysis for flow cytometry analysis. Water samples for bioinformatic analysis of phytoplankton and bacterioplankton were filtered through 0.22 μm Millipore cellulose filters (Milford, USA). The filtered membranes were then kept at -86°C until DNA extraction. The remaining water

https://doi.org/10.5194/egusphere-2025-156
Preprint. Discussion started: 7 March 2025

samples for analysis of environmental parameters were pretreated according to standard methods.

2.2. Physicochemical parameters

Water temperature (WT), dissolved oxygen (DO), and pH were measured on-site with a multiparameter sonde (YSI®EXO2, USA). The concentrations of chlorophyll a (Chl-a) and different forms of nitrogen and phosphorus in water were measured according to the Monitoring Analysis Method of Water and Wastewater (SEPA, 2002) using a UV-visible spectrophotometer (Shimadzu® UV2700i, Japan).

Concentrations of CH_4 and CO_2 in the water phase were measured with the headspace equilibration method (Goldenfum, 2010). In brief, a water sample (200 mL) was gently collected using a polypropylene syringe equipped with a three-way valve. 100 mL N_2 (99.999%) gas was added to the syringe to create a headspace. After 3 min of vigorous shaking, the equilibrated headspace gas was injected into a pre-evacuated airbag (Delin® 300 mL, Dalian) for storage until measurement. Gas samples were then analyzed using a stable isotope analyzer (Picarro® G2201-i, USA). The CH_4 and CO_2 emission fluxes at the water-air interface were estimated by the thin boundary layer method (Goldenfum, 2010). All measurements were performed in triplicate for quality assurance.

The frozen filtered POC membranes were dried at 65 °C for 48 h, fumigated with HCl (12 M) for 12 h to remove particulate inorganic carbon, and wrapped in a tin boat. The wrapped filtered POC membranes were used to analyze the concentrations of POC and PON using a stable isotope mass spectrometer coupled with an elemental

https://doi.org/10.5194/egusphere-2025-156
Preprint. Discussion started: 7 March 2025

analyzer (Thermo Fisher Scientific® Flash HT-Delta V Advantage, USA).

2.3. Analysis of microbial communities

Picophytoplankton and heterotrophic bacteria abundance (< 2 μm) in collected samples was determined using a flow cytometer (Beckman Coulter® CytoFLEX, USA). Based on previous methods (Lu et al., 2018; Yang et al., 2019), we pretreated flow cytometry samples and set the discriminator of flow cytometry. Briefly, for picophytoplankton enumeration, 1 mL of unstained sample was taken for analysis. The discriminator was set on two red and one orange fluorescence, respectively. For heterotrophic bacteria enumeration, 20 μL samples were diluted into 1 mL with sterilized water and stained with SYBR Green I (Molecular Probes, USA) for 15 min at room temperature in the dark. The discriminator was set on red and green fluorescence, respectively. Detailed flow cytometry analysis of picophytoplankton and heterotrophic bacteria was described in supplementary method S1.

Genomic DNA was extracted and duplicated from the filters with a DNA isolation kit (Mo Bio laboratories® FastDNA SPIN kit, USA) according to the manufacturer's instructions. The duplicate DNA extracts were mixed for the following PCR amplification. The primers used for the phytoplankton 23S rRNA gene were A23SrVF2 and A23SrVR2 (Yoon et al., 2016). The primers used for bacterioplankton 16S rRNA gene were 338F and 806R (Ding et al., 2020). Amplicons were purified with an AxyPrep DNA Gel Extraction Kit (Axygen Biosciences, USA). The PCR products of each sample were sequenced on the Illumina MiSeq platform at Majorbio Bio-Pharm Technology, Co., Ltd. (Shanghai, China). DNA extraction, PCR

https://doi.org/10.5194/egusphere-2025-156
Preprint. Discussion started: 7 March 2025

amplification, and high-throughput sequencing were discussed in detail in the supplementary method S2.

2.4. Stable carbon isotopic analysis

$\delta^{13}C$ of CH_4 and CO_2 in the water phase were analyzed using a stable isotope analyzer (Picarro® G2201-i, USA). Stable isotopes of POC and PON were measured using a stable isotope mass spectrometer coupled with an elemental analyzer (Thermo Fisher Scientific® Flash HT-Delta V Advantage, USA). $\delta^{13}C$ and $\delta^{15}N$ of POM were used to determine the contributions of different sources of POC. Stable isotope values of endmembers (C3 plant, C4 plant, coastal soil, and plankton) were summarized in Table S3. DOC concentration and δ^{13}-DOC were analyzed by a total organic carbon analyzer-stable isotope mass spectrometer (Elementar® vario cube TOC-isoprime100, Germany).

In this study, we applied isotopic analysis to specifically explore the impact of organic carbon from autochthonous sources on extreme values of CH_4 and CO_2 production. We focused on the two main mechanisms affecting $\delta^{13}C$-CH_4 and $\delta^{13}C$-CO_2: (i) physical proces and (ii) biological processes (Han et al., 2018). Our analysis concentrated on the variability of CH_4 and CO_2 in the water column, rather than at the air-water interface, using isotope data. We made the assumption that the fractionation effect induced by CH_4 and CO_2 exchange at the air-water interface, such as dissolution and emission, can be ignored.

https://doi.org/10.5194/egusphere-2025-156
Preprint. Discussion started: 7 March 2025

2.5. Identification of extreme and normal levels of CH_4 and CO_2 concentrations and fluxes

Pearson type III probability distribution curve (Hosking and Wallis, 1997), a widely used probability distribution function in hydrology and meteorological statistics (Sun and Qin, 1989), such as frequency analysis of extreme hydrological events, risk assessment of extreme climate, etc. (Raynal Villaseñor, 2021). Here, we employed Pearson type III probability distribution to determine the extreme and normal values of CH_4 and CO_2 concentrations and fluxes. This method allowed us to calculate the threshold values for extreme values of CH_4 and CO_2 concentrations and fluxes at 10% and 90% probabilities (Ding and Jiang, 2009). Based on these threshold values, we divided the dataset into three groups, i.e. extremely high (Ext_h), normal (nor), and extremely low (Ext_l). The supplementary material method S3 provided threshold values and sample numbers for the above three groups of CH_4 and CO_2 concentrations and fluxes, respectively.

2.6. Statistical analysis

Originpro (OriginLab®, USA, education version) was used for graphing. Data analyses were performed by SPSS (IBM, USA). Differences among groups were considered to be statistically significant if $p < 0.05$. Multiple linear regression analysis was conducted to determine whether the main predictor of carbon extreme values was POCauto or POCallo.

The trophic state of each sampling site was evaluated based on the trophic level index (TLI) (Tang et al., 2023). Alpha diversity (Shannon-Wiener and Chao1 index)

https://doi.org/10.5194/egusphere-2025-156
Preprint. Discussion started: 7 March 2025

was calculated by using the *vegan* package. The contributions of different sources to POC were estimated using Bayesian stable isotope mixing models with the *simmr* package (Parnell et al., 2013). The co-occurrence networks of phytoplankton and bacterioplankton were constructed by 16S rRNA and 23S rRNA microbial ASVs using *igraph* package. The main predictors for the abundance of picophytoplankton and heterotrophic bacteria were identified by random forest (RF) analysis with the *randomForest* package. Structure equation modeling (SEM) analysis was implemented by the *lavaan* package to explore the relationships among all variables for both the extreme and normal groups. All these methods mentioned above were described in detail in the supplementary material methods. The setting of the sampling campaign and analysis of water samples were described in our prior research (Tang et al., 2023). All data analyzed in this study are sourced from the same dataset (Tang et al., 2023).

3. Results

3.1. Identification of extreme and normal values of carbon concentrations and fluxes

The extreme and normal values for CH_4 and CO_2 concentrations and fluxes are shown in Table 1. The mean CH_4 concentration (CCH_4) in the normal and extremely high groups were 0.03±0.00 and 0.19±0.02 μmol·L^{-1}, respectively. The mean CH_4 flux (FCH_4) in the extremely low, normal, and extremely high groups were 0.01±0.00, 0.10±0.01, and 0.61±0.14 mmol·m^{-2}·d^{-1}, respectively. The mean CCO_2 in the extremely high and normal groups were 6.23 and 3.51 times higher than in the extremely low group, respectively. The mean FCO_2 in the extremely low, normal, and

https://doi.org/10.5194/egusphere-2025-156
Preprint. Discussion started: 7 March 2025

extremely high groups were 0.05±0.83, 25.72±1.16 and 62.71±8.56 mmol·m^{-2}·d^{-1}, respectively. Differences in CH_4 and CO_2 concentrations and fluxes between extreme and normal groups were significant ($p < 0.001$). Since the CH_4 concentration in the whole dataset was higher than the threshold value for the extremely low CH_4 concentration (0.004 μmol·L^{-1}), the number of samples corresponding to the extremely low group of CH_4 concentration was 0. Thus, the extremely low group (Ext_l) of CH_4 concentration (CCH_4) was nonexistent.

The trophic levels were noticeably different between extreme and normal groups of CH_4 and CO_2 concentrations and fluxes (Table 2). The TLI values in the extremely high group of CCH_4 and FCH_4 were higher than 46.27, which belonged to the eutrophic state. The TLI values fluctuated within 38.91-46.27 in the normal group of CCH_4 and FCH_4, indicating the water in the normal group was mesotrophic. With the increase of trophic state, CCH_4 and FCH_4 exhibited a increasing trend, and CCH_4 and FCH_4 ranged from 0.07 to 0.20 μmol·L^{-1} and 0.06 to 0.18 mmol·m^{-2}·d^{-1}, respectively (Fig. S3). Both extremely high and extremely low groups of CCO_2 and FCO_2 were eutrophic, but the normal group was mesotrophic (Table 2). CCO_2 and FCO_2 decreased from oligotrophic state to eutrophic state, and CCO_2 and FCO_2 ranged from 44 to 43 μmol·L^{-1} and 24 to 23 mmol·m^{-2}·d^{-1}, respectively (Fig. S3).

Ternary plots showed that the extremely high values of CCH_4 mainly occurred in July, with a relative percentage up to 56%, than in other months (relative percentage of 44% in May and 0% in November), while most of the normal values of CCH_4 appeared in November, accounting for 38% of total normal groups (Fig. 2A). We

https://doi.org/10.5194/egusphere-2025-156
Preprint. Discussion started: 7 March 2025

further observed that the extremely low, normal, and extremely high values of FCH_4 mainly occurred in November, May, and July, respectively. On the contrary, the extremely low, normal, and extremely high values of CCO_2 and FCO_2 mainly occurred in July, May, and November, respectively. These results all exhibited that extreme level of carbon concentrations and fluxes (extremely high values for CH_4 and extremely low values for CO_2) mostly appeared in July, which supports the inference that cell aggregation mediated by the PP-HB interaction drives the extreme values of CH_4 and CO_2, especially during the summer blooming period.

As Fig. 2B shows, most environmental parameters differed significantly among extremely low, normal, and extremely high groups of CH_4 and CO_2 concentrations and fluxes, with $p < 0.05$. Except for WT and POC, other environmental factors did not show significant differences among the extreme and normal groups of CCH_4 and FCH_4. The mean WT and POC exhibited an increasing trend from the extremely low to extremely high group of CCH_4 and FCH_4 ($p < 0.05$).

Results also showed that the mean NO_3^--N concentration in the normal group of CCO_2 and FCO_2 was significantly higher than that in the extremely low group of CCO_2 and FCO_2 (Fig. 2B; $p < 0.01$). An increasing trend in mean SRP concentration was observed sequentially from the extremely low to the extremely high group of CCO_2 and FCO_2, and the mean SRP was lowest in the extremely low group (0.02 $mg \cdot L^{-1}$ for CCO_2; 0.02 $mg \cdot L^{-1}$ for FCO_2) and highest in the extremely high group (0.07 for CCO_2 $mg \cdot L^{-1}$; 0.07 $mg \cdot L^{-1}$ for FCO_2); conversely, the mean DO, WT, pH were highest in the extremely low group and lowest in the extremely high group of

https://doi.org/10.5194/egusphere-2025-156
Preprint. Discussion started: 7 March 2025

CCO_2 and FCO_2. Moreover, POC and DOC in the extreme groups (high or low) of CCO_2 were higher than those in the normal group.

3.2. Contributions of autochthonous and allochthonous POC

The concentrations of autochthonous POC (POCauto) and allochthonous POC (POCallo) were noticeably different among the extreme and normal groups of CH_4 (CCH_4) and CO_2 concentrations (CCO_2) (Fig. S4). The POCauto and POCallo concentrations in whole dataset respectively ranged from 0.004 to 0.859 $mg \cdot L^{-1}$ and 0.05 to 1.77 $mg \cdot L^{-1}$, and were positively correlated with TLI (Figs. S4 and S5). In the extreme and normal groups of CCH_4, mean concentrations of POCauto and POCallo in the extremely high group (0.22±0.08 $mg \cdot L^{-1}$ for POCauto; 0.46±0.14 $mg \cdot L^{-1}$ for POCallo) were significantly higher than those in the normal groups (0.07±0.02 $mg \cdot L^{-1}$ for POCauto; 0.30±0.05 $mg \cdot L^{-1}$ for POCallo) (Fig. S4). In the extreme and normal groups of CCO_2, mean POCauto and POCallo concentrations in the extremely low groups were significantly higher than those in the normal groups (Fig. S4).

Furthermore, POCauto and POCallo were both positively correlated with the CCH_4, respectively (Fig. 3A). In the extremely high group of CCH_4, we observed a greater slope value between POCauto and CCH_4 than that between POCallo and CCH_4. However, in the normal group of CCH_4, the slope value between POCallo and CCH_4 was higher than that between POCauto and CCH_4. Statistical analysis showed that CCO_2 was significantly positively correlated with POCauto, but the relationships between CCO_2 and POCallo were not significant (Fig. 3B). The slope values between POCauto and CCO_2 were greater than those between POCallo and CCO_2 among the

https://doi.org/10.5194/egusphere-2025-156
Preprint. Discussion started: 7 March 2025

three groups. The increase in the autochthonous POC contributed to a higher CCH_4 (Fig. 3C) and lower CCO_2 (Fig. 3D), respectively.

3.3. Picophytoplankton and heterotrophic bacteria abundance across extreme and normal groups

The abundances of picophytoplankton (PP) and heterotrophic bacteria (HB) varied with extreme and normal groups of CO_2 and CH_4 concentrations (Fig. 4). The abundance of PP and HB respectively ranged from 0.01×10^5 to 5.66×10^5 cells·mL^{-1} and 0.26×10^5 to 8.90×10^5 cells·mL^{-1} in the whole dataset (Fig. 4). The difference in PP or HB abundance between extremely high (Ext_h) and normal groups (Nor) of CH_4 concentration was not significant (Fig. 4A). The HB abundance was higher than that of PP in the high (Ext_h) and normal groups (Ext_h) of CH_4 concentration (Fig. 4B). The differences in HB abundance were not significant in three extreme and normal groups of CCO_2 (Fig. 4C). The mean PP abundance in the extremely low group (Ext_l) of CO_2 concentration was significantly higher than those in the normal (Nor) and extremely high groups (Ext_h) of CO_2 concentration. The HB abundance was higher than that of PP in the extremely high (Ext_h) and normal groups (Nor) of CO_2 concentration except in the extremely low group (Ext_l) of CO_2 concentration (Fig. 4D).

We used random forest (RF) modeling (Fig. 5) to identify the main environmental predictors of picophytoplankton and heterotrophic bacteria abundance. The main environmental predictors influencing PP abundance were TP, SRP, DIN, NO_3^--N, Chl-a, DO, WT, pH, POC, and DOC ($p < 0.05$) (Fig. 5A). The main

https://doi.org/10.5194/egusphere-2025-156
Preprint. Discussion started: 7 March 2025

environmental predictors also had a certain influence on the HB abundance ($p < 0.05$) (Fig. 5B). The variance explanation of environmental factors for the abundance of PP (R^2=0.82) was higher than that of HB (R^2=0.39).

3.4. Interactions between phytoplankton and bacterioplankton communities

The co-occurrence patterns of phytoplankton and bacterioplankton in the extreme and normal groups of CH_4 and CO_2 concentrations were determined using network analysis (Fig. 6; Table 3). Overall, the number of nodes ranged from 101 to 184 in all five interaction networks. Most networks consisted of more than 50% positive edges, except in networks for the normal group of CO_2 concentration. In addition, topological properties of the co-occurrence network in normal groups of CH_4 and CO_2, such as modularity, were higher than those in the extreme groups. In contrast, the average degree showed an exactly opposite trend. The number of phytoplankton-bacterioplankton links decreased from 977 in the extremely high group to 104 in the normal group of CH_4 concentration (Fig. 6A and B). Similarly, the number of phytoplankton-bacterioplankton links in the normal group was also significantly lower than both in the extremely high and extremely low groups of CO_2 concentration (Fig. 6C-E). Compared with communities in normal groups, communities in the extreme groups exhibited a higher interaction strength (that is, links) between phytoplankton and bacterioplankton.

3.5. Influential pathways of planktonic communities on CH_4 and CO_2 concentrations

We conducted structural equation modeling (SEM) to understand the direct and

https://doi.org/10.5194/egusphere-2025-156
Preprint. Discussion started: 7 March 2025

412 indirect relationships between microbial variables and POC with CH_4 and CO_2
413 concentrations for extreme and normal groups (Fig. 7). Our SEMs explained 96 and
414 21% of the variance in CH_4 concentrations in the extremely high and normal groups,
415 respectively (Fig. 7A and B). In the extremely high group of CH_4 concentration, CH_4
416 concentration was directly influenced by picophytoplankton (PP), autochthonous POC
417 (POCauto), and allochthonous POC (POCallo) with path coefficients of 0.77, 0.35
418 and -0.26, respectively (Fig. 7A). Picophytoplankton could also indirectly affect the
419 extremely high CH_4 concentration by influencing POCauto and POCallo. POCauto
420 and POCallo were positively and negatively correlated with the extremely high CH_4
421 concentration ($p < 0.01$ and $p < 0.001$, respectively). However, HB didn't show a
422 significant influence on the extremely high CH_4 concentration. In the normal group
423 (Fig. 7B), both POCauto and POCallo were positively correlated with the CH_4
424 concentration ($p < 0.001$ and $p < 0.01$, respectively), and the path coefficient between
425 POCallo and CH_4 concentration was greater than that between POCauto and CH_4
426 concentration. However, Chl-a had a negatively direct effect on the normal value of
427 CH_4 concentration with a negative path coefficient of 0.58 ($p < 0.01$).

428 The selected variables explained 85, 26, and 96% of the variance in CO_2
429 concentrations in the three groups, respectively (Fig. 7C-E). In the extremely high
430 group of CO_2 concentration, POCauto, POCallo, and HB were not correlated with the
431 CO_2 concentration, while PP significantly affected the extremely high CO_2
432 concentration ($p < 0.001$) (Fig. 7C). In the normal group of CO_2 concentration, only
433 POCallo had a positively direct impact on the normal value of CO_2 concentration

https://doi.org/10.5194/egusphere-2025-156
Preprint. Discussion started: 7 March 2025

(p<001) (Fig. 7D). There was only one indirect path in which PP affected the normal value of CO_2 concentration by influencing POCallo. In the extremely low group of CO_2 concentration, except for POCallo, PP, POCauto, and HB showed a significant direct impact on the extremely low value of CO_2 concentration (Fig. 7E, $p < 0.001$, respectively). PP significantly affected POCauto ($p < 0.01$) and ultimately affected the extremely low value of CO_2 concentration.

4. Discussion

4.1. Contributions of POC from different sources to CH_4 and CO_2

CH_4 and CO_2 are the dominant gaseous end products of organic carbon (OC) decomposition (Yvon-Durocher et al., 2011), but the potential for CH_4 and CO_2 production and emissions differs between different sources of POC (Berberich et al., 2020). In the present study, we hypothesized that (1) the extreme values of CH_4 (CCH_4) and CO_2 concentrations (CCO_2) will mainly be fueled by autochthonous POC (POCauto), (2) the normal values of CH_4 and CO_2 concentrations will mainly be stimulated by allochthonous POC (POCallo).

Previous studies proved that autochthonous OC will decompose faster than allochthonous OC, thus sustaining higher CO_2 and CH_4 production rates than allochthonous OC (Grasset et al., 2018). This evidence probably supports the view that autochthonous POC supports short-term carbon production and emissions. Our study found steeper slopes between carbon (CH_4 and CO_2) concentrations and autochthonous POC than those between carbon concentrations and allochthonous POC in the extreme groups of CH_4 and CO_2 (Fig. 3A and B). There was more positive

https://doi.org/10.5194/egusphere-2025-156
Preprint. Discussion started: 7 March 2025

correlation between autochthonous POC and the extreme values of CH_4 and CO_2 concentrations than those between allochthonous POC and the extreme values of carbon (Table 4), indicating the main contribution of autochthonous POC to the extreme values of CH_4 and CO_2 concentrations. The evidence from isotope analysis further proved and highlighted that the extreme values of CH_4 and CO_2 concentrations were strongly influenced by autochthonous POC (Fig. 8). Photosynthesis and decomposition were the important biological processes controlling concentrations and isotope values of OC and carbon. The input of OC to reservoirs is a complex mixture of autochthonous OC (i.e., OC derived from aquatic primary production) and allochthonous OC (i.e., OC derived from terrigenous input) (Chen et al., 2021). In the extreme group of CH_4 concentration, POC in the surface water was mainly from aquatic plankton, and the average δ^{13}C-POC was approximately -26.34‰ (Table S3). Phytoplankton provides a large amount of autochthonous POC through photosynthesis, and picophytoplankton was therefore significantly correlated with POC ($p < 0.01$, Fig. 8A). However, in summer, phytoplankton may assimilate HCO_3^- as an inorganic C source under CO_2 limitation during intense photosynthesis, which weakens the discrimination of ^{13}C and enriches organic matter with ^{13}C (Fogel and Cifuentes, 1993). The above reasoning explained why the ^{13}C enrichment in the surface water DOC with the increase of the Chl-a ($p < 0.01$, Fig. 8B). A positive correlation between δ^{13}C-POC and CH_4 concentration in the extremely high group of CH_4 ($p < 0.05$, Fig. 8C) indicated that the extreme value of CH_4 was influenced by the decomposition of autochthonous POC. This is probably because the decomposition of

https://doi.org/10.5194/egusphere-2025-156
Preprint. Discussion started: 7 March 2025

OC from phytoplankton preferentially releases ^{12}C and leaves the residual OC enriched in ^{13}C (van Breugel et al., 2005). High productivity may also convert lakes or reservoirs from a CO_2 source to a sink (Balmer and Downing, 2011). The $\delta^{13}C$-DOC showed a negative correlation with $\delta^{13}C$-CO_2 ($p < 0.01$, Fig. 8D), which could be explained by an increase in phytoplankton photosynthesis (Fig. S6). These results supported the first hypothesis above.

Nevertheless, because allochthonous POC accounts for large proportions of aquatic ecosystems, allochthonous POC can support long-term CCH_4 accumulation and emissions (Berberich et al., 2020). Correspondingly, we found steeper slopes between CCH_4 and allochthonous POC than between CCH_4 and autochthonous POC in the normal group of CCH_4 (Fig. 3A). The results of SEM also highlighted that the normal values of CCH_4 and CCO_2 were positively influenced by allochthonous POC (Fig. 7B and D). These results supported our second hypothesis above.

There are two main reasons why POC from different sources have varying impacts on carbon production and emissions. First, chemical structure. Autochthonous OC, mainly composed of protein and aliphatic compounds, has relatively simple chemical structure (Kendall et al., 2001). Allochthonous POC, mainly composed of cellulose, has relatively complex chemical structure (Sondergaard and Middelboe, 1995). Second, biological availability. Complete degradation of allochthonous POC requires many species with different degradation capabilities, and therefore, the degradation of allochthonous POC is relatively slow, and the yield of carbon is stable (Grasset et al., 2018). In contrast, autochthonous POC, such as algal biomass, a labile

https://doi.org/10.5194/egusphere-2025-156
Preprint. Discussion started: 7 March 2025

carbon source, is easily available for microorganisms (Berberich et al., 2020), thus making the decomposition of autochthonous POC relatively rapid and the yield of carbon production variable. In a word, autochthonous POC can stimulate the production of extreme values of CH_4 and CO_2 in the short term (low probability of occurrence), while allochthonous POC can maintain the normal production of CH_4 and CO_2 in the long term (high probability of occurrence).

4.2. Response of picophytoplankton and heterotrophic bacteria to trophic state

Compared to oligotrophic and mesotrophic states, the eutrophic state can provide more resources for phytoplankton and bacterioplankton, thus reducing resource competition between different species (Tang et al., 2023). In this study, we found that the abundances of both picophytoplankton and heterotrophic bacteria in the extreme groups of CCH_4_Ext_h and CCO_2_Ext_l (eutrophic state) were slightly higher than those in the normal groups of CH_4 and CO_2 concentrations (mesotrophic state) (Fig. 4; Table 2; Fig. S7). Recent studies reported that the environments with sufficient resources will reduce niche overlap and enhance coexistence (Pastore et al., 2021). Niche overlap reflects the degree to which species share the factor controlling their growth (such as resources) (Pastore et al., 2021), and low niche overlap is mainly considered weaker competition (Clavel et al., 2011). Our results showed a decrease in the niche overlap of phytoplankton and bacterioplankton from oligotrophic state to eutrophic state (Fig. S8), which agrees with Clavel et al. (2011). Furthermore, in freshwater ecosystems, environmental conditions determine community diversity (Meng et al., 2020). Alpha diversity is considered positively dependent on

https://doi.org/10.5194/egusphere-2025-156
Preprint. Discussion started: 7 March 2025

environmental filters (Stefanidou et al., 2020). The increase in the alpha diversity index was mainly considered as a signal of improved trophic state (Arab et al., 2019). In our study, we found a decrease in alpha diversity of both phytoplankton and bacterioplankton from oligotrophic state to eutrophic state (Fig. S9), which agrees with Meng et al. (2020).

Bacterial taxa tended to be divided into r-strategists and K-strategists according to the preference of different OC decomposition (Li et al., 2021). Previous studies reported that the fast-growing bacterial taxa (r-strategists) prefer a environment enriched with labile C, while the slow-growing bacterial taxa (K-strategists) favor a nutrient-poor environment (Dai et al., 2022). In this study, an increase in the proportion of r-strategists to K-strategists with trophic states (Fig. S10) suggested that high eutrophic state provided more autochthonous POC (Fig. S5), promoting the growth of r-strategists. In aquatic ecosystems, picophytoplankton and heterotrophic bacteria have tiny sizes and rapid growth rates and can be characterized as typical competitors (r-strategists). Phytoplankton communities have simplex richness predominated by competitors in eutrophic lakes and rivers (Raffoul et al., 2020). In parallel, prior studies reported that picophytoplankton (PP) contributes 50-90% of primary productivity (Poulton et al., 2006), and HB consumes 20-60% of the total primary production (Williams, 1981).

Types of interactions between two species include positive relationships (such as mutualism and commensalism) and negative relationships (such as competition and amensalism) (Faust and Raes, 2012). Our results showed that in co-occurrence

https://doi.org/10.5194/egusphere-2025-156
Preprint. Discussion started: 7 March 2025

networks, the eutrophic communities displayed the highest positive interaction strength between phytoplankton and bacterioplankton compared with the oligotrophic and mesotrophic communities (Figs. 6 and S11). Such an increase supported the inference that the eutrophic state increased the interaction strength between PP and HB. Increased cell density of PP in the eutrophic state (Fig. S7) would reduce the distance between PP and HB (Petrou, 2023), and therefore increase the encounter rates and interactions in the extracellular microenvironment (Christie-Oleza et al., 2017).

4.3. Extreme and normal patterns of carbon emissions driven by picophytoplankton and heterotrophic bacteria

Although some extreme CO_2 and CH_4 air-water fluxes could be induced by short-term physical processes, the short-term physical processes were not the focus of our study. We found that water temperature showed no difference between normal and extreme groups of CO_2 fluxes (Fig. 2B). Yet, the picophytoplankton abundance in the extremely low group of CO_2 concentration was significantly higher than that in the normal group of CO_2 concentration (Fig. 4C). These results suggested that the extreme and normal values of CH_4 and CO_2 were probably influenced by ecosystem response (such as microbial community composition or abundance variation), rather than physical factors (such as temperature and wind).

In aquatic systems, the growth and functions of microorganisms are influenced mainly by the quantity and quality of substrates (Yang et al., 2023) entering the water. Microbial communities, therefore, structure their responses to OC using different life

https://doi.org/10.5194/egusphere-2025-156
Preprint. Discussion started: 7 March 2025

strategies (Delgado-Baquerizo et al., 2016), which impact water C dynamics. Previous studies reported that microbial community composition is correlated with substrate utilization strategy (Schutter and Dick, 2001). The response of microorganisms to OC from different sources is different on a time scale. Based on the growth rate and effectiveness of C utilization, microbial communities can be classified into two ecological functional groups, r- and K-selected species. Picophytoplankton and heterotrophic bacteria, as r-strategists, have a fast growth rate and a rapid response to labile C (Li et al., 2021). In contrast, K-selected species are slow-growing, decompose recalcitrant C more efficiently, and respond slowly to OC inputs. This could explain why the extreme values of CH_4 and CO_2 concentrations were positively influenced by picophytoplankton (Fig. 7). Hence, picophytoplankton and heterotrophic bacteria play essential roles in maintaining short-term extreme carbon emissions.

Our study found a significant positive correlation between network degree (interaction strength) and CH_4 concentrations in the eutrophic state (Fig. S12). Such a positive correlation corresponds to the third hypothesis that increased interaction between picophytoplankton and heterotrophic bacteria promoted the extreme values of carbon. This is mainly because positive interaction (i.e., cooperation) produces strong coupling and positive feedback between PP and HB (Coyte et al., 2015), increasing microbial metabolic efficiency and full utilization of OC. Picophytoplankton and heterotrophic bacteria have numerous enzymes for depolymerizing fresh labile C (such as autochthonous OC) (Li et al., 2021) and typically flourish in environments enriched in unstable C.

https://doi.org/10.5194/egusphere-2025-156
Preprint. Discussion started: 7 March 2025

Extremely values of CH_4 and CO_2 concentrations and fluxes were found in July (Fig. 2A). During the algal blooming period, increased cell density of PP (Fig. S7) wound enhance the possibility of "physical interaction" between phytoplankton and heterotrophic bacteria (Christie-Oleza et al., 2017). The increase in PP-HB interaction facilitates cell aggregation, increasing carbon flux export to the bottom water column, and providing sufficient substrate for CH_4 production in the bottom layer (Gärdes et al., 2011). Meanwhile, increased cell aggregation reduces respiration and CO_2 production in the upper water column (Hopkinson and Vallino, 2005). These could explain why a higher positive interaction strength (number of links) between phytoplankton and bacterioplankton was found in extreme carbon groups compared with normal groups (Fig. 6). Hence, autochthonous OC critically influenced the fate of extreme values of CH_4 and CO_2 through the interaction between PP and HB.

5. Conclusion

In the upper Yangtze's river-reservoir system, the normal CH_4 and CO_2 concentrations and fluxes were primarily contributed by the large input of allochthonous OC. In contrast, the extreme values of CH_4 and CO_2 concentrations and fluxes were mainly contributed by autochthonous OC. The picophytoplankton and heterotrophic bacteria and their interactions were important ecological factors and processes affecting extreme values of CH_4 and CO_2. Intensified interactions between PP and HB, due to an increase in the trophic state, which strongly controlled the generation and decomposition of autochthonous POC, concomitantly promoting the extreme production and emissions of CH_4 and CO_2. Our findings provide a new

https://doi.org/10.5194/egusphere-2025-156
Preprint. Discussion started: 7 March 2025

mechanism based on the interaction of picophytoplankton and heterotrophic bacteria, which would contribute to a deeper understanding of extreme carbon emissions in the river-reservoir ecosystem.

Supplements

Supplementary material associated with this article can be found on the additional files.

Data availability

The raw sequencing data has been deposited to the National Center for Biotechnology Information (NCBI) Sequence Read Archive (SRA) database under the following BioProject accession numbers: PRJNA1188301 for 23S rRNA sequencing data (http://www.ncbi.nlm.nih.gov/bioproject/1188301) and PRJNA1188367 for 16S rRNA sequencing data (http://www.ncbi.nlm.nih.gov/bioproject/1188367).

Author contributions

ZL conceived this study and acquired the research funds. LL provided genome sequence data. YX supervised the flow cytometry analysis. ZL and DW conceptualized the study. FL, QT, YX and LL process data. FL and QT conducted formal analysis. CL and XW assisted with the analysis. FL wrote the manuscript. ZL revised the manuscript. All authors approved the manuscript.

https://doi.org/10.5194/egusphere-2025-156
Preprint. Discussion started: 7 March 2025

Competing interests

The contact author has declared that none of the authors has any competing interests.

Disclaimer

Publisher's note: Copernicus Publications remains neutral with regard to jurisdictional claims made in the text, published maps, institutional affiliations, or any other geographical representation in this paper. While Copernicus Publications makes every effort to include appropriate place names, the final responsibility lies with the authors.

Acknowledgements

We acknowledge all of the partner projects listed in the financial support. We also thank Mr. Wei Tan, Ms. Xin Chen, and Mr. Qi Zhang who participated in sample collection and conducted laboratory analysis of water samples.

Financial support

This research was supported by the National Key Research and Development Program (2022YFC3203504). The National Natural Science Foundation of China (Project No. U2340222) also provided funding support.

References

Amin, S.A., Parker, M.S., Armbrust, E.V., 2012. Interactions between diatoms and bacteria. Microbiol. Mol. Biol. Rev. 76, 667-684. https://doi.org/10.1128/mmbr.00007-12.

https://doi.org/10.5194/egusphere-2025-156
Preprint. Discussion started: 7 March 2025

649 Arab, S., Hamil, S., Rezzaz, M.A., Chaffai, A., Arab, A., 2019. Seasonal variation of
650 water quality and phytoplankton dynamics and diversity in the surface water of
651 Boukourdane Lake, Algeria. Arab. J. Geosci. 12, 29.
652 https://doi.org/10.1007/s12517-018-4164-4.
653 Balmer, M.B., Downing, J.A., 2011. Carbon dioxide concentrations in eutrophic lakes:
654 undersaturation implies atmospheric uptake. Inland Waters. 1, 125-132.
655 https://doi.org/10.5268/IW-1.2.366.
656 Bauduin, T., Gypens, N., Borges, A.V., 2024. Seasonal and spatial variations of
657 greenhouse gas (CO_2, CH_4 and N_2O) emissions from urban ponds in Brussels.
658 Water Res. 253, 121257. https://doi.org/10.1016/j.watres.2024.121257.
659 Baxter, R.M., 1977. Environmental Effects of Dams and Impoundments. Annu. Rev.
660 Ecol. S. 8, 255-283. https://doi.org/10.1146/ANNUREV.ES.08.110177.001351.
661 Berberich, M.E., Beaulieu, J.J., Hamilton, T.L., Waldo, S., Buffam, I., 2020. Spatial
662 variability of sediment methane production and methanogen communities within
663 a eutrophic reservoir: Importance of organic matter source and quantity. Limnol.
664 Oceanogr. 65, 1336-1358. https://doi.org/10.1002/lno.11392.
665 Chen, S., Zhong, J., Li, S.L., Ran, L.S., Wang, W.F., Xu, S., Yan, Z.L., Xu, S., 2021.
666 Multiple controls on carbon dynamics in mixed karst and non-karst mountainous
667 rivers, Southwest China, revealed by carbon isotopes ($\delta^{13}C$ and $\Delta^{14}C$). Sci. Total
668 Environ. 791, 148347. https://doi.org/10.1016/j.scitotenv.2021.148347.
669 Christie-Oleza, J.A., Sousoni, D., Lloyd, M., Armengaud, J., Scanlan, D.J., 2017.
670 Nutrient recycling facilitates long-term stability of marine microbial
671 phototroph–heterotroph interactions. Nat. Microbiol. 2, 17100.
672 https://doi.org/10.1038/nmicrobiol.2017.100.
673 Clavel, J., Julliard, R., Devictor, V., 2011. Worldwide decline of specialist species:
674 toward a global functional homogenization? Front. Ecol. Environ. 9, 222-228.
675 https://doi.org/10.1890/080216.
676 Coyte, K.Z., Schluter, J., Foster, K.R., 2015. The ecology of the microbiome:
677 Networks, competition, and stability. Science 350, 663-666.
678 https://doi.org/10.1126/science.aad2602.
679 Dai, T., Wen, D., Bates, C.T., Wu, L., Guo, X., Liu, S., Su, Y., Lei, J., Zhou, J., Yang,
680 Y., 2022. Nutrient supply controls the linkage between species abundance and
681 ecological interactions in marine bacterial communities. Nat. Commun. 13, 175.
682 https://doi.org/10.1038/s41467-021-27857-6.
683 Delgado-Baquerizo, M., Maestre, F.T., Reich, P.B., Jeffries, T.C., Gaitan, J.J., Encinar,
684 D., Berdugo, M., Campbell, C.D., Singh, B.K., 2016. Microbial diversity drives
685 multifunctionality in terrestrial ecosystems. Nat. Commun. 7, 10541.
686 https://doi.org/10.1038/ncomms10541.
687 Ding, C., Adrian, L., Peng, Y., He, J., 2020. 16S rRNA gene-based primer pair showed
688 high specificity and quantification accuracy in detecting freshwater Brocadiales
689 anammox bacteria. FEMS Microbiol. Ecol. 96, fiaa013.
690 https://doi.org/10.1093/femsec/fiaa013.
691 Ding, Y.G., Jiang, Z.H., 2009. Introduction to extreme climate research methods.
692 China Meteorological Press, Beijing.

https://doi.org/10.5194/egusphere-2025-156
Preprint. Discussion started: 7 March 2025

Durham, B.P., Sharma, S., Luo, H., Smith, C.B., Amin, S.A., Bender, S.J., Dearth, S.P., Van Mooy, B.A.S., Campagna, S.R., Kujawinski, E.B., Armbrust, E.V., Moran, M.A., 2015. Cryptic carbon and sulfur cycling between surface ocean plankton. Proc. Natl. Acad. Sci. USA. 112, 453-457. https://doi.org/10.1073/pnas.14131371.

Emilson, E.J.S., Carson, M.A., Yakimovich, K.M., Osterholz, H., Dittmar, T., Gunn, J.M., Mykytczuk, N.C.S., Basiliko, N., Tanentzap, A.J., 2018. Climate-driven shifts in sediment chemistry enhance methane production in northern lakes. Nat. Commun. 9, 1801. https://doi.org/10.1038/s41467-018-04236-2.

Faust, K., Raes, J., 2012. Microbial interactions: from networks to models. Nat. Rev. Microbiol. 10, 538-550. https://doi.org/10.1038/nrmicro2832.

Fogel, M.L., Cifuentes, L.A., 1993. Isotope fractionation during primary production. Springer. Berlin.

Gärdes, A., Iversen, M.H., Grossart, H.P., Passow, U., Ullrich, M.S., 2011. Diatom-associated bacteria are required for aggregation of *Thalassiosira weissflogii*. ISME J. 5, 436-445. https://doi.org/10.1038/ismej.2010.145.

Goldenfum J.A., 2010. GHG measurement guidelines for freshwater reservoirs. In: International Hydropower Association (Eds.), The UNESCO/IHA Greenhouse Gas Emissions from Freshwater Reservoirs Research. IHA, London, pp. 72-77.

Grasset, C., Mendonça, R., Saucedo, G.V., Bastviken, D., Roland, F., Sobek, S., 2018. Large but variable methane production in anoxic freshwater sediment upon addition of allochthonous and autochthonous organic matter. Limnol. Oceanogr. 63: 1488-1501. https://doi.org/10.1002/lno.10786.

Guillemette, F., McCallister, S.L., del Giorgio, P.A., 2013. Differentiating the degradation dynamics of algal and terrestrial carbon within complex natural dissolved organic carbon in temperate lakes. J. Geophys. Res-Bioge. 118, 963-973. https://doi.org/10.1002/jgrg.20077.

Han, Q., Wang, B.L., Liu, C.Q., Wang, F., Peng, X., Liu, X.L., 2018. Carbon biogeochemical cycle is enhanced by damming in a karst river. Sci. Total Environ. 616, 1181-1189. https://doi.org/10.1016/j.scitotenv.2017.10.202.

Hopkinson, C.S., Vallino, J.J., 2005. Efficient export of carbon to the deep ocean through dissolved organic matter. Nature 433, 142-145. https://doi.org/10.1038/nature03191.

Hosking, J.R.M., Wallis, J.R., 1997. Regional frequency analysis: an approach based on L-moments, Cambridge University Press, Cambridge.

IPCC, 2021. Climate change 2021: The physical science basis. In: Masson-Delmotte, V., Zhai, P., Pirani, S.L., Connors, S.L., Péan, C., Berger, S., Caud, N., Chen, Y., Goldfarb, L., Gomis, M.I., Huang, M., Leitzell, K., Lonnoy, E., Matthews, J.B.R., Maycock, T.K., Waterfield, T. Yelekçi, O., Yu, R., Zhou, B. (Eds.), Contribution of working group I to the sixth assessment report of the intergovernmental panel on climate change. Cambridge University Press, Cambridge.

Irion, S., Christaki, U., Berthelot, H., L'Helguen, S., Jardillier, L., 2021. Small phytoplankton contribute greatly to CO_2-fixation after the diatom bloom in the Southern Ocean. ISME J. 15, 2509-2522.

https://doi.org/10.5194/egusphere-2025-156
Preprint. Discussion started: 7 March 2025

https://doi.org/10.1038/s41396-021-00915-z.
Kendall, C., Silva, S.R., Kelly, V.J., 2001. Carbon and nitrogen isotopic compositions of particulate organic matter in four large river systems across the United States. Hydrol. Process. 15, 1301-1346. https://doi.org/10.1002/hyp.216.
Li, H., Yang, S., Semenov, M.V., Yao, F., Ye, J., Bu, R., Ma, R., Lin, J., Kurganova, I., Wang, X., Deng, Y., Kravchenko, I., Jiang, Y., Kuzyakov, Y., 2021. Temperature sensitivity of SOM decomposition is linked with a K-selected microbial community. Glob Chang Biol 27, 2763-2779. https://doi.org/10.1111/gcb.15593.
Liikanen, A., Tanskanen, H., Murtoniemi, T., Martikainen, P., 2002. A laboratory microcosm for simultaneous gas and nutrient flux measurements in sediments. Boreal. Environ. Res. 7, 151-160. https://www.researchgate.net/publication/242309730_A_laboratory_microcosm_for_simultaneous_gas_and_nutrient_fl_ux_measurements_in_sediments.
Lu, L., Xu, L., Yang, J., Li, Z., Guo, J., Xiao, Y., Yao, J., 2018. Contribution of heterotrophic bacterioplankton to cyanobacterial bloom formation in a tributary backwater area of the Three Gorges Reservoir, China. Environ. Sci. Pollut. Res. Int. 25, 27402-27412. https://doi.org/10.1007/s11356-018-2790-8.
Maavara, T., Chen, Q., Van Meter, K., Brown, L.E., Zhang, J., Ni, J., Zarfl, C., 2020. River dam impacts on biogeochemical cycling. Nat. Rev. Earth Environ. 1, 103-116. https://doi.org/10.1038/s43017-019-0019-0.
Malfatti, F., Azam, F., 2009. Atomic force microscopy reveals microscale networks and possible symbioses among pelagic Marine Bacteria. Aquat. Microb. Ecol. 58, 1-14. https://doi.org/10.3354/ame01355.
Meng, F., Li, Z., Li, L., Lu, F., Liu, Y., Lu, X., Fan, Y., 2020. Phytoplankton alpha diversity indices response the trophic state variation in hydrologically connected aquatic habitats in the Harbin Section of the Songhua River. Sci. Rep. 10, 21337. https://doi.org/10.1038/s41598-020-78300-7.
Parnell, A.C., Phillips, D.L., Bearhop, S., Semmens, B.X., Ward, E.J., Moore, J.W., Jackson, A.L., Grey, J., Kelly, D.J., Inger, R., 2013. Bayesian stable isotope mixing models. Environmetrics 24, 387-399. https://doi.org/10.1002/env.2221.
Pastore, A.I., Barabás, G., Bimler, M.D., Mayfield, M.M., Miller, T.E., 2021. The evolution of niche overlap and competitive differences. Nat Ecol Evol. 5, 330-337. https://doi.org/10.1038/s41559-020-01383-y.
Petrou, K., 2023. Phytoplankton-bacteria interactions 2.0. Microorganisms, 11, 1536. https://doi.org/10.3390/microorganisms11061536.
Poulton, A.J., Holligan, P.M., Hickman, A., Kim, Y.N., Adey, T.R., Stinchcombe, M.C., Holeton, C., Root, S., Woodward, E.M.S., 2006. Phytoplankton carbon fixation, chlorophyll-biomass and diagnostic pigments in the Atlantic Ocean. Deep-Sea Res. Pt. II 53, 1593-1610. https://doi.org/10.1016/j.dsr2.2006.05.007.
Raffoul, M.H., Enanga, E.M., E Senar, O., Creed, I.F., Trick, C.G., 2020. Assessing the potential health risk of cyanobacteria and cyanotoxins in Lake Naivasha, Kenya. Hydrobiologia 847, 1041-1056. https://doi.org/10.1007/s10750-019-04167-z.
Raynal Villaseñor, J.A., 2021. Frequency analyses of natural extreme events. Springer,

https://doi.org/10.5194/egusphere-2025-156
Preprint. Discussion started: 7 March 2025

Berlin.
Richardson, T.L., 2019. Mechanisms and pathways of small-phytoplankton export from the surface ocean. Ann. Rev. Mar. Sci. 11, 57-74. https://doi.org/10.1146/annurev-marine-121916-063627.
Schutter, M., Dick, R., 2001. Shifts in substrate utilization potential and structure of soil microbial communities in response to carbon substrates. Soil Biol. Biochem. 33, 1481-1491. https://doi.org/10.1016/S0038-0717(01)00057-8.
SEPA., 2002. The Monitoring Analysis Method of Water and Waste Water, 4th ed. China Environmental Science Press, Beijing.
Seymour, J.R., Amin, S.A., Raina, J.B., Stocker, R., 2017. Zooming in on the phycosphere: the ecological interface for phytoplankton–bacteria relationships. Nat. Microbiol. 2, 17065. https://doi.org/10.1038/nmicrobiol.2017.65.
Sieburth, J., Smetacek, V., Lenz, J., 1978. Pelagic ecosystem structure: Heterotrophic compartments of the plankton and their relationship to plankton size fractions. Limnol. Oceanogr. 23, 1256-1263. https://doi.org/10.4319/lo.1978.23.6.1256.
Sondergaard, M., Middelboe, M., 1995. A cross-system analysis of labile dissolved organic carbon. Mar Ecol Prog Ser. 118, 283-294. https://doi.org/10.3354/meps118283.
Stockner, J.G., 1988. Phototrophic picoplankton: An overview from marine and freshwater ecosystems. Limnol Oceanogr. 33, 765-775. https://doi.org/10.4319/lo.1988.33.4part2.0765.
Stockner, J.G., Antiam, N., J., 1986. Algal picoplankton from marine and freshwater ecosystems: a multidisciplinary perspective. Can. J. Fish. Aquat. Sci. 43, 2472-2503. https://doi.org/10.1139/f86-307.
Sun, H., Lu, X., Yu, R., Yang, J., Liu, X., Cao, Z., Zhang, Z., Li, M., Geng, Y., 2021. Eutrophication decreased CO_2 but increased CH_4 emissions from lake: A case study of a shallow Lake Ulansuhai. Water Res. 201, 117363. https://doi.org/10.1016/j.watres.2021.117363.
Sun, J.L., Qin, D.Y., 1989. Study on the general model of hydrological frequency analysis. J. Hydraul. Eng. 24, 1-10. https://doi.org/10.13243/j.cnki.slxb.1989.04.001.
Tang, Q., Lu, L.H., Luo, F., Li, X.R., Zhang, Y.Y., Li, R., Bernal, C., Vera, S., Izaguirre, I., Xiao, Y., Li, Z., 2023. Terrigenous organic carbon contributes to reservoir carbon emissions: Potential role of the microbial community along a trophic gradient. J. Hydrol. 621, 129601. https://doi.org/10.1016/j.jhydrol.2023.129601.
Thornton, K.W., Kimmel, B.L., Payne, F.E., 1990. Reservoir limnology: ecological perspectives. John Wiley & Sons, Hoboken.
van Breugel, Y., Schouten, S., Paetzel, M., Nordeide, R., Sinninghe Damsté, J.S., 2005. The impact of recycling of organic carbon on the stable carbon isotopic composition of dissolved inorganic carbon in a stratified marine system (Kyllaren fjord, Norway). Org. Geochem. 36, 1163-1173. https://doi.org/10.1016/j.orggeochem.2005.03.003.
Wang, W., Zeng, C.S., Tong, C., 2008. Methane production and oxidation capacities

https://doi.org/10.5194/egusphere-2025-156
Preprint. Discussion started: 7 March 2025

of soil from the reed marsh of the Minjiang River estuary. Wetland Science 6, 60-68. https://doi.org/10.13248/j.cnki.wetlandsci.2008.01.012.

Williams, P.J., 1981. Incorpooration of microheterotrophic processes into the classical paradigm of the planktonic food web. Kieler Meeresforsch-Sonderh 5, 1-28. Available from https://oceanrep.geomar.de/id/eprint/56172.

Woyke, T., Teeling, H., Ivanova, N.N., Huntemann, M., Richter, M., Gloeckner, F.O., Boffelli, D., Anderson, I.J., Barry, K.W., Shapiro, H.J., Szeto, E., Kyrpides, N.C., Mussmann, M., Amann, R., Bergin, C., Ruehland, C., Rubin, E.M., Dubilier, N., 2006. Symbiosis insights through metagenomic analysis of a microbial consortium. Nature 443, 950-955. https://doi.org/10.1038/nature05192.

Yang, Y., Dou, Y., Wang, B., Xue, Z., Wang, Y., An, S., Chang, S.X., 2023. Deciphering factors driving soil microbial life-history strategies in restored grasslands. iMeta. 2, e66. https://doi.org/10.1002/imt2.66.

Yang, Y., Gu, X.Q., Te, S.H., Goh, S.G., Mani, K., He, Y.L., Gin, K.Y.H., 2019. Occurrence and distribution of viruses and picoplankton in tropical freshwater bodies determined by flow cytometry. Water Res. 149, 342-350. https://doi.org/10.1016/j.watres.2018.11.022.

Yoon, T.H., Kang, H.E., Kang, C.K., Lee, S., Ahn, D.H., Park, H., Kim, H.W., 2016. Development of a cost-effective metabarcoding strategy for analysis of the marine phytoplankton community. PeerJ 4, e2115. https://doi.org/10.7717/peerj.2115.

Yvon-Durocher, G., Montoya, J.M., Woodward, G.U.Y., Jones, J.I., Trimmer, M., 2011. Warming increases the proportion of primary production emitted as methane from freshwater mesocosms. Global Change Biol. 17, 1225-1234. https://doi.org/10.1111/j.1365-2486.2010.02289.x.

Zhang, Z., Nair, S., Tang, L., Zhao, H., Hu, Z., Chen, M., Zhang, Y., Kao, S.J., Jiao, N., Zhang, Y., 2021. Long-Term Survival of Synechococcus and Heterotrophic Bacteria without External Nutrient Supply after Changes in Their Relationship from Antagonism to Mutualism. mBio 12, e01614-21. https://doi.org/10.1128/mbio.01614-01621.

Zhou, Y.T., Li, J.L., Zhao, Z.J., Qi, S., 2022. Research progress on the interaction between marine picocyanobacteria and heterotrophic bacteria. Marine Sciences 46, 123-132. https://doi.org/10.11759/hykx20210805002.

https://doi.org/10.5194/egusphere-2025-156
Preprint. Discussion started: 7 March 2025

Figures

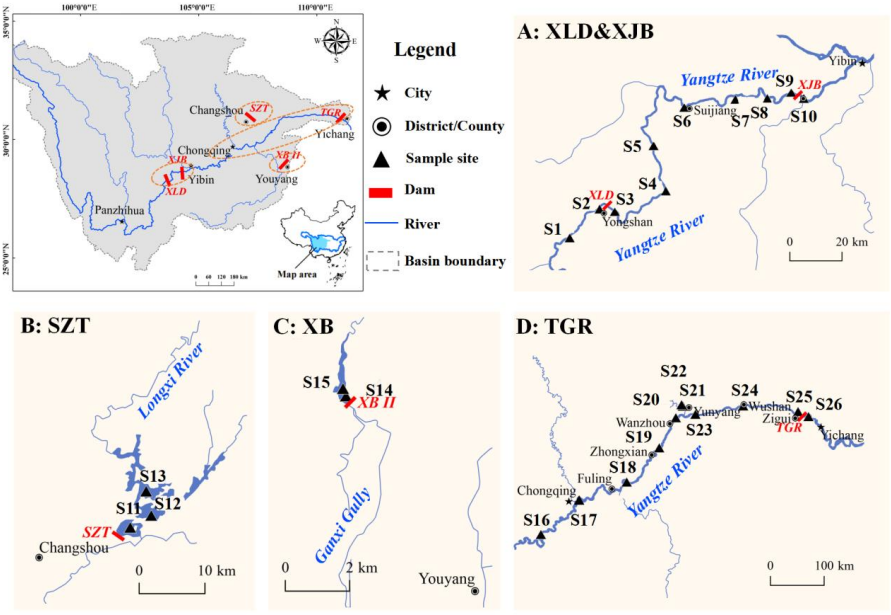

Fig. 1. Location of sampling sites in five reservoirs in the upper Yangtze River. Detailed information on sampling sites in five reservoirs is shown in Table S2.

https://doi.org/10.5194/egusphere-2025-156
Preprint. Discussion started: 7 March 2025

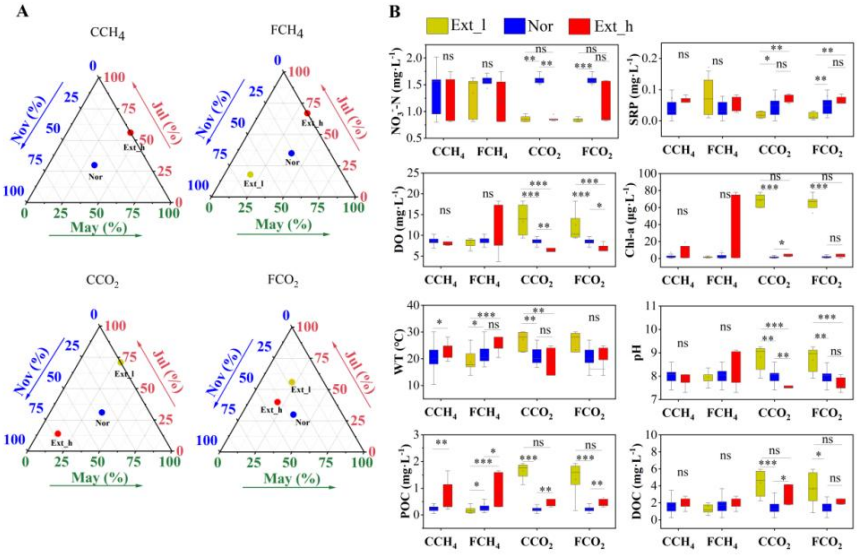

Fig. 2. Comparison of months and environmental parameters in extreme and normal groups. Panel A Ternary plots showing the percentage of months (May, July, and November) in which the extremely low (Ext_l), normal (Nor), and extremely high (Ext_h) values of CH_4 and CO_2 concentrations and fluxes occurred. The yellow, blue, and red dots represent the Ext_l, Nor, and Ext_h groups. Panel B Characteristics of NO_3^--N, SRP, DO, Chl-a, WT, pH, POC, and DOC in surface water. The yellow, blue, and red boxes represent environmental parameters in the extremely low (Ext_l), normal (Nor), and extremely high (Ext_h) groups of CH_4 and CO_2 concentrations and fluxes, respectively. Asterisks indicate significant difference: * $p < 0.05$, ** $p < 0.01$, *** $p < 0.001$.

https://doi.org/10.5194/egusphere-2025-156
Preprint. Discussion started: 7 March 2025

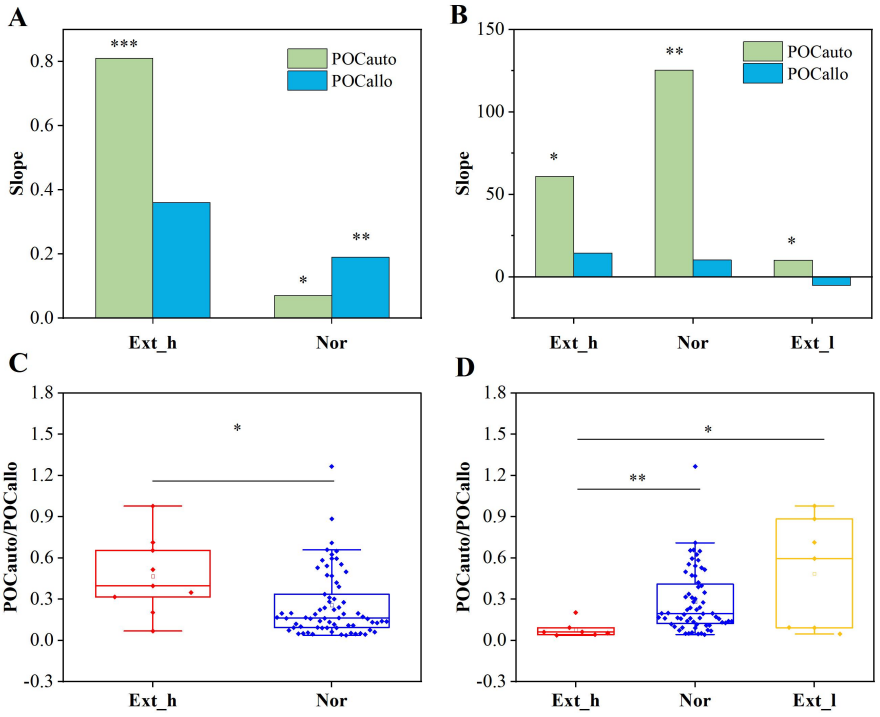

Fig. 3. Panels A and B Slope values of POC concentrations (autochthonous POC, allochthonous POC) linear regression analysis with carbon concentrations (CCH_4, CCO_2) in extremely high (Ext_h), normal (Nor) and extremely low (Ext_l) group, respectively. Panels C and D The concentration ratio of autochthonous POC to allochthonous POC (POCauto/POCallo) in extremely high (Ext_h), normal (Nor) and extremely low (Ext_l) groups of CCH_4 and CCO_2. Asterisks above the bar chart and box plot indicate significant levels: * $p < 0.05$, ** $p < 0.01$, *** $p < 0.001$.

https://doi.org/10.5194/egusphere-2025-156
Preprint. Discussion started: 7 March 2025

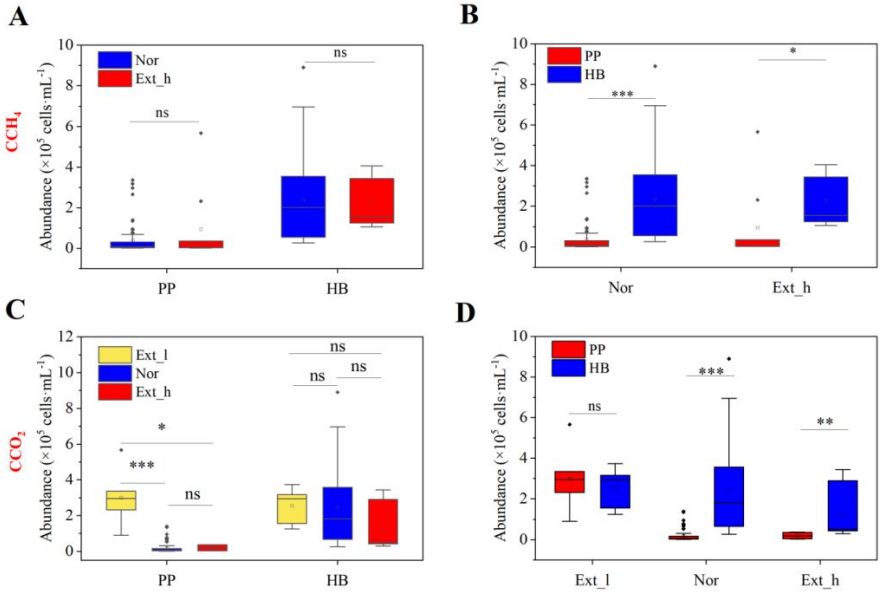

Fig. 4. Abundance of picophytoplankton and heterotrophic bacteria in the extremely high (Ext_h), normal (Nor) and extremely low (Ext_l) groups of CH_4 (A, B) and CO_2 (C, D) concentrations.

https://doi.org/10.5194/egusphere-2025-156
Preprint. Discussion started: 7 March 2025

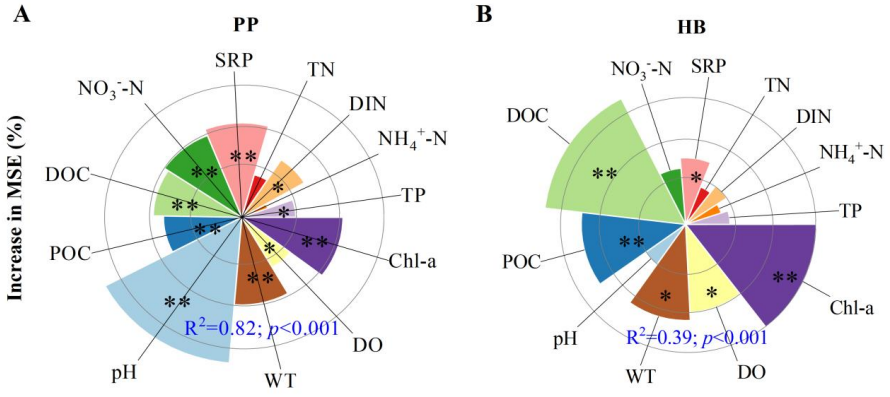

Fig. 5. Environmental predictors of picophytoplankton (A) and heterotrophic bacteria abundance (B). Random forest modelling importance of environmental predictors on picophytoplankton and heterotrophic bacteria abundance were estimated by percentage increases in the mean squared error (%IncMSE). Significance levels of each predictor are as follow: * $p < 0.05$ and ** $p < 0.01$.

https://doi.org/10.5194/egusphere-2025-156
Preprint. Discussion started: 7 March 2025

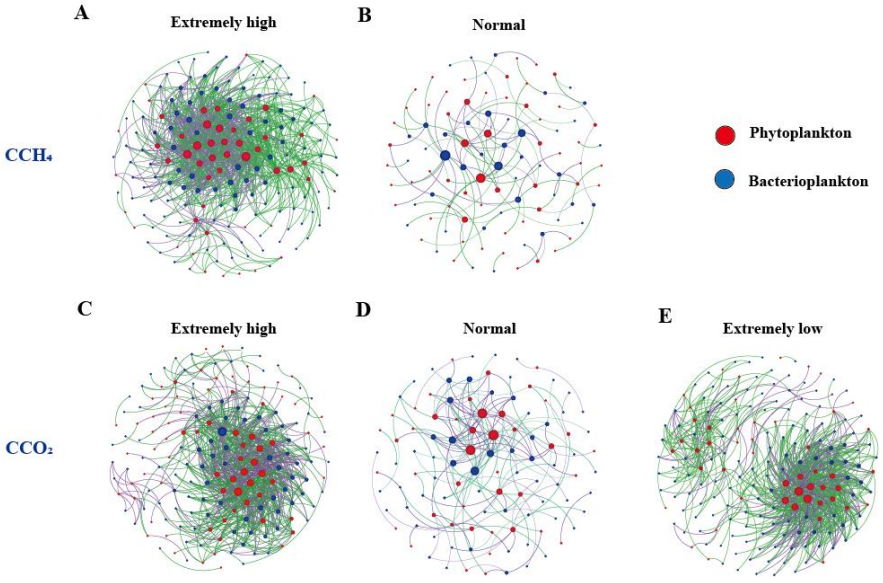

Fig. 6. Co-occurrence networks of phytoplankton and bacterioplankton communities based on correlation analysis. Panels A and B Co-occurrence patterns of phytoplankton-bacterioplankton interaction network in extremely high and normal groups of CH_4 concentration (CCH_4). Panels C, D, and E Co-occurrence patterns of phytoplankton-bacterioplankton interaction network in extremely high, normal, and extremely low groups of CO_2 concentration (CCO_2). Each line represents a significant correlation between the two taxa, with the green lines representing positive correlations and the violet lines representing negative correlations. The number of links represents the strength of interactions between phytoplankton and bacterioplankton. The red and blue nodes in each network represent phytoplankton and bacterioplankton, respectively. The size of each node is proportional to the number of connections (that is, degree).

https://doi.org/10.5194/egusphere-2025-156
Preprint. Discussion started: 7 March 2025

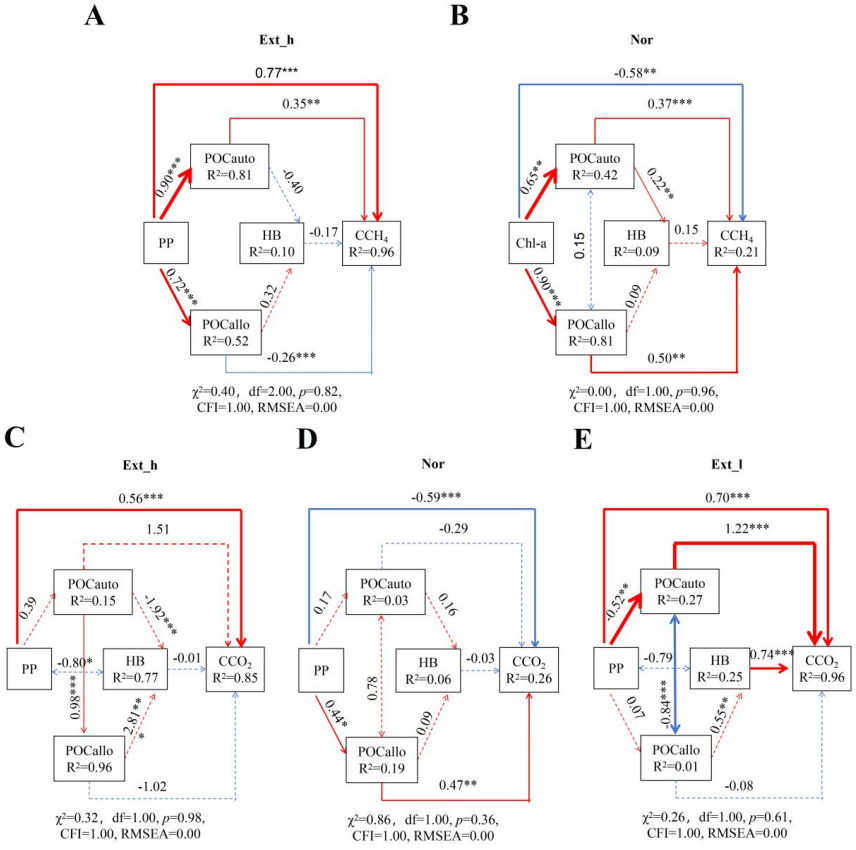

Fig. 7. Structural equation modeling (SEM) describing selected variables' effects on the concentration of CH_4 (A, B) and CO_2 (C, D, E) in the extremely high (Ext_h), normal (Nor) and extremely low (Ext_l) group, respectively. Numbers adjacent to arrows are standardized path coefficients and indicative of the effect size of the relationship. Solid arrows indicate significant paths (* $p < 0.05$, ** $p < 0.01$, *** $p < 0.001$), and dashed lines represent non-significant paths. The red and blue arrows indicate positive and negative path coefficients, respectively. The width of the arrows represents the strength of relationships. R^2 denotes the percentage of variance explained by the model. PP, picophytoplankton; HB, heterotrophic bacterial; POCauto, autochthonous POC; POCallo, allochthonous POC; CCH_4 and CCO_2 were the concentrations of CH_4 and CO_2.

https://doi.org/10.5194/egusphere-2025-156
Preprint. Discussion started: 7 March 2025

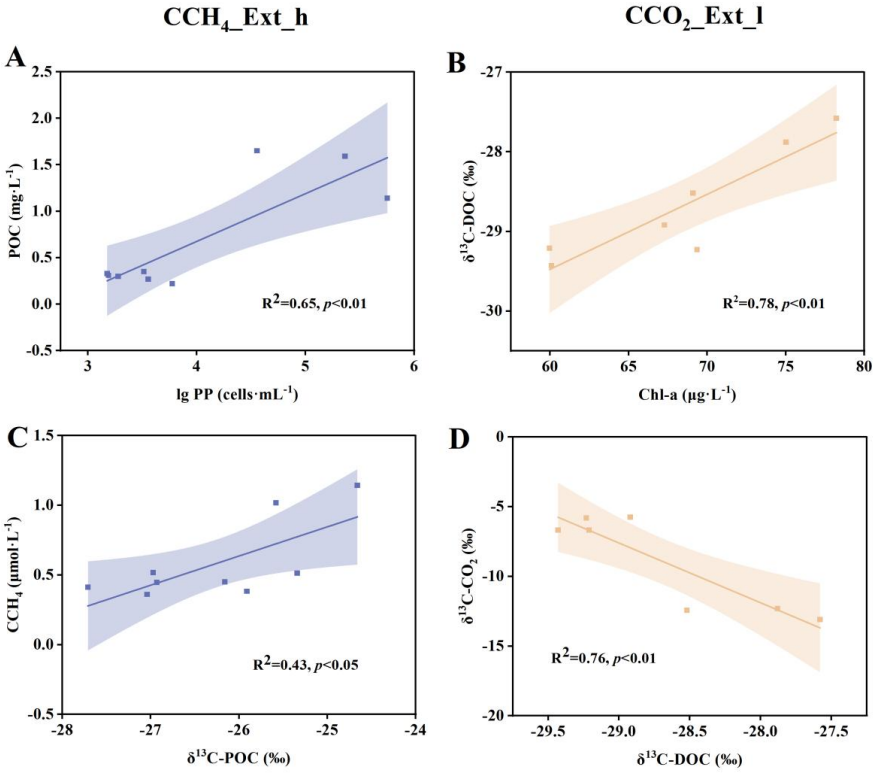

910

911 **Fig. 8.** Scatter plots of PP versus POC (A) and δ^{13}C-POC versus CCH_4 (C) in the extremely high
912 (Ext_h) group of CCH_4. Scatter plots of Chl-a versus δ^{13}C-DOC (B) and δ^{13}C-DOC versus
913 δ^{13}C-CO_2 (D) in the extremely low (Ext_l) group of CCO_2. The violet and yellow areas represent
914 95% confidence intervals.

https://doi.org/10.5194/egusphere-2025-156
Preprint. Discussion started: 7 March 2025

Tables

Table 1

Concentrations and fluxes of CO_2 and CH_4 in the extremely low (Ext_l), normal (Nor) and extremely high (Ext_h) groups.

		Mean	SE	Range	N
Ext_l	CCH_4	-	-	-	-
	FCH_4	0.01	0.00	0.01-0.02	17
	CCO_2	12.62	1.49	8.46-18.01	7
	FCO_2	0.05	0.83	-4.08-3.76	9
Nor	CCH_4	0.03	0.00	0.00-0.12	69
	FCH_4	0.10	0.01	0.03-0.29	55
	CCO_2	44.25	1.33	24.28-64.63	64
	FCO_2	25.72	1.16	7.24-42.39	64
Ext_h	CCH_4	0.19	0.02	0.13-0.33	9
	FCH_4	0.61	0.14	0.36-1.09	6
	CCO_2	78.66	2.91	71.92-92.74	7
	FCO_2	62.71	8.56	50.01-93.85	5

Note: CCH_4 and CCO_2 denote the concentrations of CO_2 and CH_4 in the surface water ($\mu mol \cdot L^{-1}$), respectively. FCH_4 and FCO_2 denote the fluxes of CH_4 and CO_2 across the water-air interface ($mmol \cdot m^{-2} \cdot d^{-1}$), respectively. -: not exist; SE: standard error; N: the number of observations.

https://doi.org/10.5194/egusphere-2025-156
Preprint. Discussion started: 7 March 2025

Table 2

TLI values in extreme and normal groups of CH_4 and CO_2 concentrations and fluxes

	Groups	Mean	SE	Range	Trophic state
	CCH_4_Ext_l	-	-	-	-
	CCH_4_Nor	44.99	1.07	33.91-70.03	M
	CCH_4_Ext_h	50.54	4.19	41.13-70.81	E
	FCH_4_Ext_l	42.04	0.95	36.96-49.14	M
	FCH_4_Nor	45.79	1.29	33.91-70.03	M
	FCH4_Ext_h	54.32	5.79	41.13-70.81	E
TLI					
	CCO_2_Ext_l	69.11	0.50	67.41-70.80	E
	CCO_2_Nor	42.39	0.69	33.91-67.87	M
	CCO_2_Ext_h	51.71	1.80	47.13-58.81	E
	FCO_2_Ext_l	62.66	4.29	39.49-70.81	E
	FCO_2_Nor	42.84	0.71	33.91-67.87	M
	FCO_2_Ext_h	50.65	3.70	38.93-58.81	E

Note: -: not exist.

https://doi.org/10.5194/egusphere-2025-156
Preprint. Discussion started: 7 March 2025

925 **Table 3**

926 Topological properties of co-occurrence network of phytoplankton-bacterioplankton interaction in
927 the extremely low (Ext_l), normal (Nor), and extremely high (Ext_h) groups of CH_4 (CCH_4) and
928 CO_2 concentrations (CCO_2).

Network metrics	CCH_4		CCO_2		
	Nor	Ext_h	Ext_l	Nor	Ext_h
Number of nodes	101	173	184	108	175
Number of edges	104	977	800	171	841
(Interaction strength)					
Number of positive edges	59	630	543	76	561
	(56.73%)	(64.48%)	(67.87%)	(44.44%)	(66.71%)
Number of negative edges	45	347	257	95	280
	(43.27%)	(35.52%)	(32.12%）	(55.56%)	(33.29%)
Modularity	0.752	0.292	0.404	0.558	0.341
Average degree	2.059	11.295	8.696	3.167	9.611

929

https://doi.org/10.5194/egusphere-2025-156
Preprint. Discussion started: 7 March 2025

930 **Table 4**

931 Results of multiple linear regression analysis relating GHGs with POC from different sources in

932 the CCH_4_ Ext_h and CCO_2_Ext_l group, respectively.

Group	Equations	R^2	*p*	Significance level	
				T-test	
				t_1	t_2
Ext_h	CH_4=1.11 (POCauto)-0.10 (POCallo)+0.38	0.74	**	4.34**	-0.61
Ext_l	$LgCO_2$=1.36[Lg(POCauto+1)]+0.29[Lg(POCallo +1)]+0.78	0.70	*	3.02*	0.55

933 **Note:** Asterisks indicate significant levels: * $p < 0.05$, ** $p < 0.01$, *** $p < 0.001$.